Electron Spin Relaxation in Chromium−Nitrosyl Complexes

Lenny M. Carruthers, Christina L. Closken, Karen L. Link, and Surendra N. Mahapatro*

Department of Chemistry, Regis University, Denver, Colorado 80221

Malavosklish Bikram, Jing-Long Du, Sandra S. Eaton, and Gareth R. Eaton

Department of Chemistry and Biochemistry, University of Denver, Denver, Colorado 80208

Received September 2, 1998

A new method to prepare $Cr(NO)(H_2O)_5^{2+}$ from dichromate and NH_2OH is reported. The chromium nitrosyls $Cr(NO)(EHBA)^+$ and $Cr(NO)(EHBA)_2$ (EHBA = 2-ethyl-2-hydoxybutyrate) were prepared by a literature reaction and characterized by continuous wave electron paramagnetic resonance and two-pulse electron spin echo spectroscopy at X-band. The *g* values are characteristic of a single unpaired electron in a predominantly d_{xy} orbital. In fluid and glassy solutions $Cr(NO)(EHBA)_2$ is a mixture of cis and trans isomers. Rotation of the methyl groups in the EHBA ligands causes an increased rate of spin echo dephasing at temperatures between 40 and 120 K. For the EHBA complexes echo envelope modulation is observed at temperatures below about 40 K that is attributed to inequivalent coupling to protons of the slowly rotating methyl groups. Both the effect of the methyl rotation on spin echo dephasing and the depth of the proton modulation are dependent on the number of ethyl groups in the ligand, and thus the spin echo experiments provide confirmation of the number of EHBA ligands in the complexes. The spin−lattice relaxation rates for the chromium−nitrosyl complexes at temperatures near 100 K are similar to values reported previously for Cr(V) complexes, which also have a single unpaired electron in a predominantly d_{xy} orbital. For $Cr(NO)(H_2O)_5^{2+}$, $Cr(NO)(EHBA)^+$, and $Cr(NO)(EHBA)_2$ the dominant contribution to spin−lattice relaxation between 12 and 150 K is the Raman process with a Debye temperature, θ_D, of 110−120 K. For $Cr(NO)(CN)_5^{3-}$ the data are consistent with a Raman process (θ_D = 135 K) and a contribution from a local mode, which dominates above about 60 K. The formally low-spin d^5 chromium nitrosyl complexes relax about 5 orders of magnitude more slowly than low-spin d^5 Fe(III) porphyrins, which is attributed to the absence of a low-lying excited state.

Introduction

Much of the early literature concerning electron spin−lattice relaxation was based on studies of ionic species in crystalline lattices, which led to descriptions of relaxation mechanisms in terms of lattice phonons. To develop models of relaxation processes in transition metal complexes and metalloenzymes in glassy solution, additional experimental data are required. We have shown previously that electron spin−lattice relaxation rates as a function of temperature between 10 and 120 K are similar for chromium(V) nitrido porphyrins[1] and oxo−chromium(V) bis(2-ethyl-2-hydroxybutyrate), $(CrO(EHBA)_2^-)$.[2−4] In view of the current interest in both chromium chemistry and the chemistry of nitric oxide, we have now examined the electron spin relaxation rates for four chromium−nitrosyl complexes, $Cr(NO)(CN)_5^{3-}$, $Cr(NO)(H_2O)_5^{2+}$, $Cr(NO)(EHBA)_2$, and $Cr(NO)(EHBA)^+$.

Ardon and Herman prepared $Cr(NO)(H_2O)_5^{2+}$ by the reaction of chromous perchlorate with nitrate or nitric oxide, purified it by ion exchange chromatography, and characterized it by IR, UV−vis, and magnetic susceptibility measurements.[5] The preparation was subsequently confirmed by Griffith.[6] We describe a new method of preparation of $Cr(NO)(H_2O)_5^{2+}$ by reaction of NH_2OH with dichromate.

Rajasekar et al. obtained two products from the reductive nitrosylation reaction between hydroxylamine and oxo−chromium(V) bis(2-ethyl-2-hydroxybutyrate), $(CrO(EHBA)_2^-)$.[7] On the basis of the kinetics of the reaction, elution from an ion exchange column, and visible and infrared spectroscopy, the products were identified as $Cr(NO)(EHBA)_2$ and $Cr(NO)(EHBA)^+$.[7] We now provide additional characterization of the products based on continuous wave and time domain EPR.

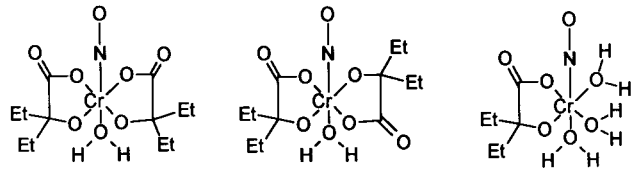

Experimental Section

$CrO(EHBA)_2^-$ [8] and $Cr(NO)(CN)_5^{3-}$ [9] were prepared by literature methods. The reaction between NH_2OH and $CrO(EHBA)_2^-$ and subsequent separation of $Cr(NO)(EHBA)_2$ and $Cr(NO)(EHBA)^+$ by ion

(1) Konda, R.; Du, J.-L.; Eaton, S. S.; Eaton, G. R. *Appl. Magn. Reson.* **1994**, *7*, 185−193.
(2) Nakagawa, K.; Candelaria, M. B.; Chik, W. W. C.; Eaton, S. S.; Eaton, G. R. *J. Magn. Reson.* **1992**, *98*, 81−92.
(3) Du, J.-L.; Eaton, G. R.; Eaton, S. S. *J. Magn. Reson. A* **1995**, *115*, 236−240.
(4) Abbreviations: CrNTTP, nitridochromium(V) tetratolylporphyrin; CrTPP(NO), chromium tetraphenylporphyrin nitrosyl; EHBA, 2-ethyl-2-hydroxybutyrate dianion.
(5) Ardon, M.; Herman, J. *J. Chem. Soc.* **1962**, 507−509.
(6) Griffith, W. P. *J. Chem. Soc.* **1963**, 3286−3289.

10.1021/ic981063+ CCC: $18.00
Published on Web 06/30/1999

Table 1. EPR Parameters for Chromium−Nitrosyls and Related Chromium(V) Complexes

complex	g_{iso}	A^{Cr}_{iso} (G)	A^{N}_{iso}[a] (G)	g_x	g_y	g_z	A^{Cr}_x[b] (10^{-4} cm^{-1})	A^{Cr}_y (10^{-4} cm^{-1})	A^{Cr}_z (10^{-4} cm^{-1})	ref
$Cr(NO)(H_2O)_5^{2+}$	1.968	26.0	6.3	1.998	1.998	1.916	15	15	40	*d*
$Cr(NO)(EHBA)^{+}$ [c]	1.967	26.0	6.3	1.995	1.995	1.914	16	16	39	*d*
$Cr(NO)(EHBA)_2$ [c]	1.966	26.2	6.0	1.996	1.996	1.913	16	16	39	*d*
	1.969	26.2	6.0	1.996	1.996	1.920	16	16	37	
$Cr(NO)(NH_3)_5^{2+}$	1.980	25.0	7.0	1.955	1.955	1.945				18
CrTPP(NO)	1.993	21.2	6.5	2.00	2.00	1.97				19
$Cr(NO)(CN)_5^{3-}$ [e]	1.994	18.4	5.2	2.002	2.002	1.970	11	11	32	9, *d*
$Cr(NO)(L)_5^{2+}$ [f]	1.993	18.0	4.7							20
$CrO(EHBA)_2^{-}$	1.978	18.3		1.971	1.973	1.983	5.0	34.3	6.0	3, 8
CrNTTP[g]	1.983	28.4		1.995	1.995	1.955	20.8	20.8	36.6	1, 27, 28

[a] Coupling to nitrosyl nitrogen. [b] The conversion factor between G and cm^{-1} is $A(\text{cm}^{-1}) = 4.6686 \times 10^{-5} gA(\text{G})$. [c] Coupling to nitrosyl nitrogen partially resolved on perpendicular lines $= 7.5 \times 10^{-4}$ cm^{-1}. [d] This work. [e] Coupling to nitrosyl nitrogen resolved on perpendicular lines $= 6.2 \times 10^{-4}$ cm^{-1}. [f] L is an aliphatic isocyanide. [g] Coupling to nitrido nitrogen: $A^{N}_{iso} = 2.8$ G, three components in frozen solution $= 3.4$, 3.2, and 1.2×10^{-4} cm^{-1}.

exchange chromatography were performed using the procedure of Rakasekar et al.[7]

Preparation of $Cr(NO)(H_2O)_5^{2+}$. In a typical procedure 10 mL of 0.2 M hydroxylamine perchlorate, pH 3.5, was reacted with 100 μL of 0.5 M sodium dichromate. The reaction mixture was allowed to stand at room temperature for 30 min. The visible spectrum showed a peak at 565 nm and a broad shoulder at 435 nm. The reaction mixture was loaded on a cation exchange column (Biorad AG 50W-X2 H^+ form; column length 15 cm, internal column diameter 1.5 cm). No chromium-containing fraction could be eluted with distilled water (∼50 mL). A yellow-brown fraction was eluted with 0.5 M $HClO_4$ (∼40 mL). The visible spectrum exhibits $\lambda_{max} = 564$ and 452 nm, which is in good agreement with literature values for $Cr(NO)(H_2O)_5^{2+}$: λ_{max} at 559 and 449 nm[5] or λ_{max} at 567 and 447 nm.[6] Elution with 1.0 M $HClO_4$ resulted in a second fraction with λ_{max} at 578 and 406 nm, which is characteristic of aqueous chromium(III).[10] Interestingly, if the reaction of hydroxylamine with chromic acid is performed at pH ≤ 2, there is no chromium nitrosyl EPR signal, and visible spectra indicate that the products contain only chromium(III).

EPR spectra were obtained on freshly prepared samples. After elution from the column, fractions were kept on ice for 1−2 h. Samples for room temperature EPR measurements were contained in 1 mm capillary tubes. For the low-temperature studies, glycerol was added to the solutions in 1:1 volume ratios to ensure glass formation, and samples were contained in 4 mm o.d. quartz tubes. Concentrations were 0.3−1.0 mM. There was no evidence of concentration dependence of the relaxation rates in this concentration range. Samples were stored in liquid nitrogen. Continuous wave (CW) EPR spectra were run on a Varian E9 or in the CW mode of the saturation recovery or spin echo spectrometers. Values of *g* and hyperfine coupling constants (Table 1) were determined by computer simulation using locally written programs (Epr2 for fluid solution and Monmer for rigid lattices) that include second-order corrections to the hyperfine interaction. The nitrogen hyperfine splitting along the *z* axis (estimated from the isotropic fluid solution value and the observed value in the perpendicular plane) is about 2×10^{-4} cm^{-1}, which is so small compared with line widths that it is not included in the simulations.

Electron spin echo (ESE) measurements were performed with a 90°−τ−180°−τ−echo 2-pulse sequence on a locally designed and constructed spectrometer with a Varian TE_{102} rectangular cavity resonator modified to permit overcoupling[11] or on a Bruker ESP380E or Elexsys E580 with a split ring resonator. Data were obtained with a resonator *Q* of about 150. Measurements of T_1 were performed by long-pulse saturation recovery on a locally designed and constructed spectrometer with a Varian TE_{102} resonator.[12] Sample temperatures in the liquid nitrogen range were monitored with a thermocouple in the cavity, positioned directly above the sample. Temperatures in the liquid helium range were calibrated by replacing the sample-containing tube with a tube containing a thermocouple immersed in 1:1 water/glycerol. The experimental recovery times were independent of pump time between 20 and 400 μs, which indicates that spectral diffusion was not interfering with the measurements of T_1. A pump time of 20−100 μs was used to record the data shown in Figures 5 and 6. The estimated uncertainties in $1/T_1$ are ±10%.

Spin echo data were fitted to a stretched exponential

$$Y(\tau) = Y(0)\exp[-(2\tau/T_m)^x] \qquad (1)$$

where $Y(\tau)$ is the intensity of the echo as a function of τ, the time between the two pulses. $Y(0)$, echo intensity extrapolated to time 0, and $Y(\tau)$ are in arbitrary units that depend on the concentration of the sample, resonator *Q*, and instrument settings. The parameters *x* and T_m describe the shape of the echo decay and depend on the dephasing mechanism.[13,14] Data were fitted to eq 1 using a nonlinear Levenberg−Marquardt least-squares algorithm. The decay was fitted to the peaks of shallow proton echo envelope modulation.

Values of T_1 were obtained from the saturation recovery data by fitting to a single exponential or to the sum of two exponentials. Although the fits to a sum of exponentials were slightly better than to a single exponential, the temperature dependence of T_1 for the two components was essentially the same as for T_1 obtained from the single-exponential fits. Since there is more scatter in the relaxation times obtained by fitting to two components, analysis of the temperature dependence was performed for the values obtained from the single-exponential fits. The temperature dependence of $1/T_1$ was fitted to eq 2 by minimizing the sum of the residuals on a log−log scale.

$$\frac{1}{T_1} = A_{dir}T + A_{Ram}\left(\frac{T}{\theta_D}\right)J_8\left(\frac{\theta_D}{T}\right) + A_{loc}\left[\frac{e^{\Delta_{loc}/T}}{(e^{\Delta_{loc}/T}-1)^2}\right] \qquad (2)$$

where T is temperature in kelvins, A_{dir} is the coefficient for the contribution from the direct process, A_{Ram} is the coefficient for the contribution from the Raman process, θ_D is the Debye temperature, J_8 is the transport integral, $J_8(\theta_D/T) = \int_0^{\theta_D/T} x^8[e^x/(e^x-1)^2]\,dx$, A_{loc} is the coefficient for the contribution from a local vibrational mode, and Δ_{loc} is the energy for the local mode in kelvins.

Mathematical expressions for the temperature dependence of spin−lattice relaxation are taken from the following references: Raman

(7) Rajasekar, N.; Subramaniam, R.; Gould, E. S. *Inorg. Chem.* **1983**, *22*, 971−975.
(8) Krumpolc, M.; DeBoer, D. G.; Rocek, J. *J. Am. Chem. Soc.* **1978**, *100*, 145−149.
(9) Manoharan, P. T.; Gray, H. B. *Inorg. Chem.* **1966**, *5*, 823−839.
(10) Laswick, J. A.; Plane, R. A. *J. Am. Chem. Soc.* **1959**, *81*, 3564−3567.
(11) Quine, R. W.; Eaton, G. R.; Eaton, S. S. *Rev. Sci. Instrum.* **1987**, *58*, 1709−1723.
(12) Quine, R. W.; Eaton, S. S.; Eaton, G. R. *Rev. Sci. Instrum.* **1992**, *63*, 4251−4262.
(13) Brown, I. M. In *Time Domain Electron Spin Resonance* Kevan, L., Schwartz, R. N., Eds.; Wiley: New York, 1979; Chapter 6.
(14) Lindgren, M.; Eaton, G. R.; Eaton, S. S.; Jonsson, B.-H.; Hammarström, P.; Svensson, M.; Carlsson, U. *J. Chem. Soc., Perkin Trans. 2* **1997**, 2549−2554.

Table 2. Contributions to Spin−Lattice Relaxation Determined by Fitting to Eq 2

sample	temp range (K)	g values[a]	direct A_{dir}	Raman A_{Ram}, θ_D	local A_{loc}, Δ_{loc}[b]
$Cr(NO)(CN)_5^{3-}$	10−150	2.002, 1.970		1.3×10^5, 135	1.3×10^6, 310
$Cr(NO)(H_2O)_5^{2+}$	10−160	1.998, 1.916		9.1×10^5, 110	2.0×10^5, 360[c]
$Cr(NO)(EHBA)^+$	12−160	1.995, 1.914		8.6×10^5, 120	2.8×10^5, 360[c]
$Cr(NO)(EHBA)_2$	12−130	1.996, 1.917		6.6×10^5, 110	5.6×10^5, 360[c]
$CrO(EHBA)_2^-$ [d]	10−150	1.971, 1.972, 1.983	1.3	1.3×10^5, 115	8.7×10^5, 370
CrNTTP[d]	18−130	1.994, 1.956	4.8	1.2×10^5, 135	4.3×10^5, 320

[a] For complexes with axial symmetry g values are given in the order $g_\perp$, $g_\parallel$. [b] Energies in kelvins. [c] Local mode makes small contribution at highest temperatures examined. [d] Analysis of relaxation rates was reported in ref 17.

process, ref 15, and local mode ref 16. An Orbach process was not included because there are no known low-lying electronic states for the Cr(V) or Cr(NO) complexes and an Orbach process was not required to fit the experimental data.

Strategy Used in Fitting the Experimental Data. The procedure used to analyze the temperature dependence of $1/T_1$ for the chromium−nitrosyl complexes is similar to that used previously for a series of $S = {}^1/_2$ centers.[17] For each sample the temperature dependence of $1/T_1$ was fitted with the smallest number of contributing processes consistent with the experimental data. A fit to a Raman process was attempted first.[17] Additional contributions were then added as required to match the data. The weak temperature dependence of relaxation produced by the direct process is distinctive, and its effects are negligible for the chromium−nitrosyl complexes in the temperature range examined.

The resulting best-fit parameters are given in Table 2. On the basis of the residuals from the fitting procedure, the uncertainty in the Debye temperature or in the characteristic energy for a local mode is about 10% for the dominant contribution to the relaxation rate. Errors in the Debye temperature, or in the characteristic energy for a local mode, and the coefficient for that process are correlated. For example, changing the value of θ_D from 105 to 110 K requires increasing A_{Ram} by about 15% to give approximately the same relaxation rates at 100 K. In addition, uncertainties in temperature, particularly at low temperature, could be a source of larger systematic errors. Uncertainties in fitted parameters are substantially larger for processes that make only a small contribution to the experimental relaxation rate in the temperature range examined.

Results and Discussion

The room temperature CW EPR spectrum of $Cr(NO)(H_2O)_5^{2+}$ is shown in Figure 1a. The intense lines in the center of the spectrum are due to chromium isotopes with $I = 0$, which constitutes 90.5% of natural abundance chromium. The well-resolved three-line splitting (6.3 G) is due to coupling to the nitrosyl nitrogen. The less intense lines in the wings of the spectra are due to hyperfine coupling to ^{53}Cr with $I = {}^3/_2$, which constitutes 9.5% of natural abundance chromium. The g and hyperfine parameters obtained by simulation of the spectrum are given in Table 1 and are in good agreement with values reported previously for $Cr(NO)(CN)_5^{3-}$ [9] and other well-characterized chromium−nitrosyl complexes.[18−20]

The spectrum of $Cr(NO)(EHBA)^+$ (Figure 1b) is similar to that for $Cr(NO)(H_2O)_5^{2+}$, but with slightly broader lines that may result from unresolved hyperfine splitting by protons from the EHBA ligand. The spectrum of $Cr(NO)(EHBA)_2$ (Figure 1c) is distinctly different, and simulations indicate that it is a superposition of two three-line signals with hyperfine splittings of 6.0 G and slightly different g values (Table 1). The simulation shown in Figure 1c was obtained with a 60:40 ratio of components with $g = 1.966$ and 1.969. The component with the higher g value decomposed to Cr(III) slightly more quickly than the component with the lower g value. For example, in samples of $Cr(NO)(EHBA)_2$ that had sat overnight at room temperature, the integrated signal intensity decreased by about 20% and the ratio of the two components was about 70:30.

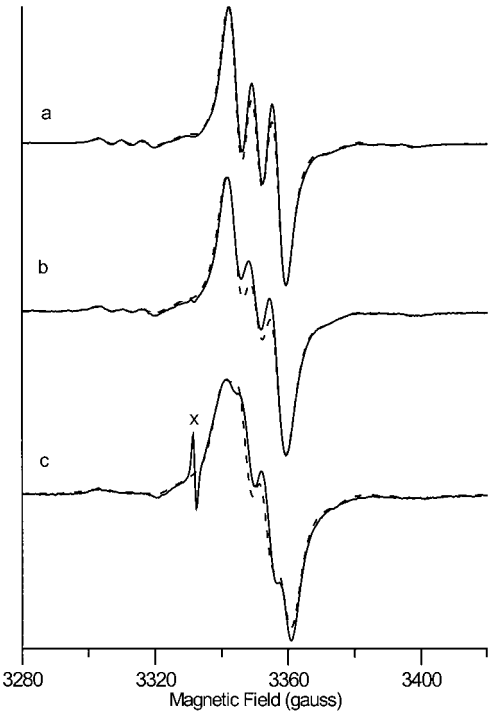

Figure 1. Continuous wave X-band (9.227 GHz) EPR spectra obtained at room temperature with 20 mW microwave power and 1.0 G modulation amplitude at 100 kHz for aqueous solutions of (a) 0.78 mM $Cr(NO)(H_2O)_5^{2+}$, (b) 0.52 mM $Cr(NO)(EHBA)^+$, and (c) 0.94 mM $Cr(NO)(EHBA)_2$. The x in part c denotes the contribution to the spectrum from a low concentration of $CrO(EHBA)_2^-$. The dashed lines show the simulations obtained with the parameters given in Table 1. The line shapes are a linear combination of 80% Gaussian and 20% Lorentzian with the following line widths: $Cr(NO)(H_2O)_5^{2+}$, 5.2 G; $Cr(NO)(EHBA)^+$, 6.3 G; and $Cr(NO)(EHBA)_2$, 5.8 G.

The CW spectrum of $Cr(NO)(H_2O)_5^{2+}$ in glassy solution at 118 K is shown in Figure 2a. The dominant features of the spectra are due to chromium isotopes with $I = 0$. In the simulations of the spectra the ^{53}Cr hyperfine coupling was defined by the low-field shoulder on the perpendicular turning point and by the highest-field line of the ^{53}Cr quartet for the parallel turning point, which is shown at expanded scale in Figure 2. The low-temperature spectrum for $Cr(NO)(EHBA)^+$ (Figure 2b) is similar to that for $Cr(NO)(H_2O)_5^{2+}$ (Figure 2a). In both spectra coupling to the nitrosyl nitrogen is barely resolved on the perpendicular turning point and not resolved on the parallel turning point. The spectrum of $Cr(NO)(EHBA)_2$ (Figure 2c) is similar to those for $Cr(NO)(H_2O)_5^{2+}$ and Cr(NO)-

(15) Murphy, J. *Phys. Rev.* **1966**, *145*, 241−247.
(16) Castle, J. G., Jr.; Feldman, D. W. *Phys. Rev. A* **1965**, *137*, 671−673.
(17) Zhou, Y.; Bowler, B. E.; Eaton, G. R.; Eaton, S. S. *J. Magn. Reson*, in press.
(18) Manoharan, P. T.; Kuska, H. A.; Rogers, M. T. *J. Am. Chem. Soc.* **1967**, *89*, 4564−4565.
(19) Wayland, B. B.; Olson, L. W.; Siddiqui, Z. U. *J. Am. Chem. Soc.* **1976**, *98*, 94−98.
(20) Wigley, D. E.; Walton, R. A. *Organometallics* **1982**, *1*, 1322−1327.

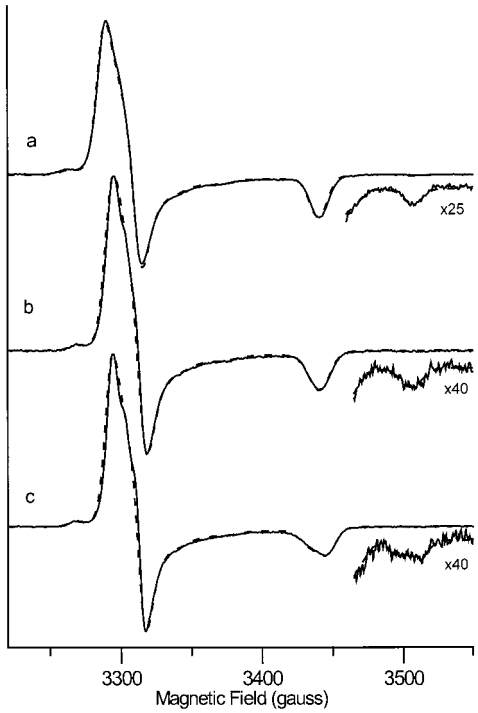

Figure 2. Continuous wave X-band (9.226 GHz) EPR spectra obtained at 118 K with 0.25 mW microwave power and 2.0 G modulation amplitude at 100 kHz for 1:1 water/glycerol solutions of (a) 0.39 mM $Cr(NO)(H_2O)_5^{2+}$, (b) 0.26 mM $Cr(NO)(EHBA)^+$, and (c) 0.47 mM $Cr(NO)(EHBA)_2$. The insets are the highest field lines of the ^{53}Cr hyperfine splitting at the $g_{||}$ turning point. The dashed lines show the simulations obtained with the parameters given in Table 1. The line shape is Gaussian, and the line widths are anisotropic, varying from 10 G in the perpendicular plane to 12−14 G along the *z* axis.

$(EHBA)^+$ except that two partially resolved components of the parallel turning point are observed for both the $I = 0$ and $I = {}^3/_2$ isotopes. The ratio of the two components is about 60:40, which is similar to the ratio observed for the two components in fluid solution.

The parameters obtained by simulation of the low-temperature spectra are in good agreement with parameters obtained for other chromium−nitrosyl complexes (Table 1); thus the EPR spectra confirm the characterization of these complexes as chromium nitrosyls. We propose that the two components observed in the room temperature and low-temperature spectra of $Cr(NO)(EHBA)_2$ are due to the presence of cis and trans isomers as has been proposed for the Cr(V) complex of the same ligand, $CrO(EHBA)_2^-$.[21]

Characterization by Two-Pulse Electron Spin Echoes. Field-swept spin-echo detected spectra at 10 K of a solution of $Cr(NO)(EHBA)_2$ that had been allowed to sit overnight at room temperature showed the signal characteristic of $Cr(NO)(EHBA)_2$ plus a broad underlying signal characteristic of Cr(III). The Cr(III) signal is sufficiently broad that it is not detected in the fluid solution room temperature spectra and is difficult to detect by CW EPR in the glassy samples. The advantage of the echo-detected spectrum is that it is the absorption spectrum, which facilitates observation of broad signals for which the first-derivative signal would be difficult to distinguish from baseline. This Cr(III) signal was absent from freshly prepared solutions. These observations are consistent with data obtained by visible spectroscopy and confirm that the chromium nitrosyls are cleanly separated form Cr(III)-containing complexes by the ion exchange chromatography. Cr(III) subsequently is produced by slow degradation of the chromium−nitrosyl complex.

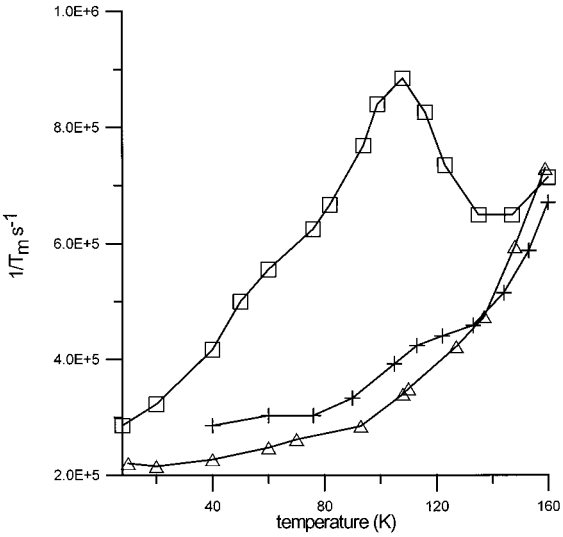

Figure 3. Temperature dependence of X-band phase memory relaxation rates, $1/T_m$, measured at the $g_\perp$ turning point in the CW spectra for 0.39 mM $Cr(NO)(H_2O)_5^{2+}$ (Δ), 0.26 mM $Cr(NO)(EHBA)^+$ (+), and for 0.47 mM $CrO(EHBA)_2^-$ (□) in 1:1 water/glycerol. The solid lines connect the data points.

The phase memory relaxation rates, $1/T_m$, in the two-pulse spin echo decays for $Cr(NO)(EHBA)_2$ are temperature dependent (Figure 3). As the temperature is increased above about 30 K, $1/T_m$ increases and then decreases. In this temperature interval the value of *x* obtained by fitting the data to eq 1 decreases from about 1.6 at 40 K to about 0.95 at 110 K and then increases with further increase in temperature up to about 130 K. Both the increase in $1/T_m$ and the decrease in *x* are characteristic of a temperature regime in which a dynamic process that averages inequivalent environments is occurring on the time scale of the splitting that is averaged by the process. A similar temperature dependence of $1/T_m$ was observed for $CrO(EHBA)_2^-$ and is assigned to rotation of the methyl groups in the ligand.[2] The maximum enhancement of $1/T_m$ is observed when the rate of rotation of the methyl group is comparable to the splitting that is averaged by the rotation. The maximum in $1/T_m$ occurs at similar temperatures for $Cr(NO)(EHBA)_2$ (Figure 3) and for $CrO(EHBA)_2^-$,[2] which is consistent with the expectation that the barrier to rotation of the methyl groups is similar for the two complexes. There are only half as many methyl groups in $Cr(NO)(EHBA)^+$ as in $Cr(NO)(EHBA)_2$ so the effect of the methyl group rotation on $1/T_m$ is expected to be only half as large, which corresponds to a maximum effect of about $4 \times 10^5\ s^{-1}$. This enhancement is relatively small compared with the contributions of other processes to the spin echo dephasing, but is consistent with the small increase in $1/T_m$ for $Cr(NO)(EHBA)^+$ at about 110 K (Figure 3). A similar maximum in $1/T_m$ near 110 K is not observed for $Cr(NO)(H_2O)_5^{2+}$, consistent with the absence of methyl groups in this complex. For all four chromium−nitrosyl complexes $1/T_m$ increases above about 120 K as mobility increases and as $1/T_1$ approaches $1/T_m$ (see below).

Two-pulse electron spin echo decays for $Cr(NO)(EHBA)^+$ and $Cr(NO)(EHBA)_2$ at 20 K (Figure 4b) exhibit modulation with a maximum impact on echo amplitude at about 0.7 μs, which corresponds to a period of about 1.4 μs and a frequency of about 0.7 MHz. The dashed line in Figure 4b indicates the shape of the decay that is estimated in the absence of the low-

(21) Branca, M.; Dessi, A.; Micera, G.; Sanna, D. *Inorg. Chem.* **1993**, *32*, 578−581.

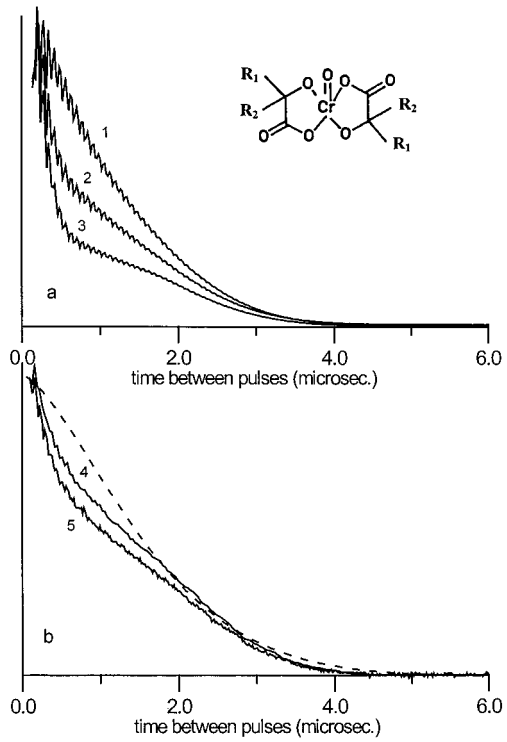

Figure 4. Two-pulse electron spin echo decays. (a) Data at 20 K in the middle of the CW spectra for 1 mM 1:1 water/glycerol solutions of Cr(V) complexes of α-hydroxy carboxylic acids with $R_1 = R_2 =$ methyl (curve 1), $R_1 =$ methyl, $R_2 =$ ethyl (curve 2), and $R_1 = R_2 =$ ethyl (curve 3) obtained with 20 and 40 ns 90° and 180° pulses. (b) Data at 8 K at the $g_\perp$ turning point for 1:1 water/glycerol solutions of 0.37 mM $Cr(NO)(EHBA)^+$ (curve 4) and 0.21 mM $Cr(NO)(EHBA)_2$ (curve 5) obtained with 40 and 80 ns 90° and 180° pulses. The dashed line is the estimated shape of the decay curve if the low-frequency proton modulation were not present. The high-frequency proton modulation is deeper in curves 1−3 than in curves 4 and 5 because of the shorter pulses that were used to obtain the data.

frequency modulation. The low-frequency modulation is deeper for $Cr(NO)(EHBA)_2$ (Figure 4b, curve 5) than for $Cr(NO)(EHBA)^+$ (Figure 4b, curve 4). This modulation is not observed in three-pulse echoes. Analogous low-frequency modulation was observed for Cr(V) complexes of EHBA.[2] Data for three Cr(V) complexes of α-hydroxy carboxylic acids (Figure 4a) show that the depth of the low-frequency modulation increases with the number of ethyl groups on the ligand. Since the modulation depth for both series of complexes increases with the number of ethyl groups, we assign the modulation to protons of the ethyl group.

Zhidomirov and Salikhov[22] calculated the electron spin echo signal for the case of a two-site dynamic process that averages coupling between the unpaired electron and two inequivalent nuclei. The coupling to the two inequivalent nuclei results in a splitting of the EPR signal that is averaged by the dynamic process. When the rate of the dynamic process is comparable to the splitting that is averaged, the equations predict an increase in $1/T_m$, analogous to what is seen for $Cr(NO)(EHBA)_2$ (Figure 3) and $CrO(EHBA)_2^-$.[2] Their model[22] also predicts that when the rate of the dynamic process is slow relative to the splitting, the splitting results in echo modulation. The equations would be more complicated for the three-site exchange due to methyl group rotation, but the principles are the same. We propose that the modulation observed at low temperature for the EHBA

(22) Zhidomirov, G. M.; Salikhov, K. M. *Sov. Phys., JETP* **1969**, *29*, 1037−1040.

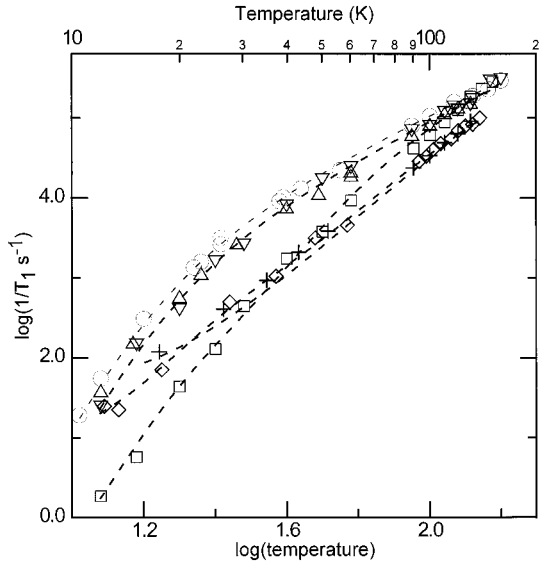

Figure 5. Temperature dependence of X-band electron spin−lattice relaxation rates, $1/T_1$, at the $g_\perp$ turning point in the CW spectra in chromium−nitrosyl complexes, compared with values for chromium(V) complexes: 0.9 mM $Cr(NO)(CN)_5^{3-}$ (□); 0.26 mM $Cr(NO)(EHBA)^+$ (▽); 0.47 mM $Cr(NO)(EHBA)_2$ (Δ); 0.39 mM $Cr(NO)(H_2O)_5^{2+}$ (○); 1 mM CrNTTP (+); 1 mM $CrO(EHBA)_2^-$ (◇). Data were obtained in 1:1 water/glycerol except that data for CrNTTP were obtained in toluene. The dashed lines are the fits of the data to eq 2 obtained with the parameters shown in Table 2.

complexes is due to interaction of the unpaired electrons with the inequivalent protons of the slowly rotating methyl groups. The splitting is the difference between couplings to inequivalent protons. For this three-site case there are likely to be several splittings that would be averaged by rapid methyl rotation and therefore several modulation frequencies. The presence of several relatively low frequencies is consistent with the rapid damping of the modulation.

Electron Spin−Lattice Relaxation. The spin−lattice relaxation rates for $Cr(NO)(H_2O)_5^{2+}$, $Cr(NO)(EHBA)^+$, $Cr(NO)(EHBA)_2$, and $Cr(NO)(CN)_5^{3-}$ were measured by long-pulse saturation recovery between 12 and 150 K. The relaxation rates measured at the perpendicular turning point in the CW spectra for the four complexes are shown in Figure 5. Included in Figure 5 are data for the chromium(V) complexes CrNTTP[1] and $CrO(EHBA)_2^-$.[2,3,17] The temperature dependence of $1/T_1$ for the chromium−nitrosyl complexes was fitted to eq 2 and the resulting parameters are given in Table 2. The values of the Debye temperatures, θ_D, for the chromium nitrosyls [$Cr(NO)(CN)_5^{3-}$, 135 K; $Cr(NO)(H_2O)_5^{2+}$, 110 K; $Cr(NO)(EHBA)^+$, 120 K; and $Cr(NO)(EHBA)_2$, 110 K] are similar to those for chromium(V) complexes [$CrO(EHBA)_2^-$, 115 K; and CrNTTP, 135 K] (Table 2) and to values for other $S = {}^1/_2$ molecules in 1:1 water/glycerol.[17] The coefficient of the contribution from the Raman process to the spin−lattice relaxation for $Cr(NO)(CN)_5^{3-}$ ($A_{Ram} = 1.3 \times 10^5$) is similar to values obtained for the Cr(V) complexes, $CrO(EHBA)_2^-$ and CrNTTP, but is substantially smaller than for $Cr(NO)(H_2O)_5^{2+}$, $Cr(NO)(EHBA)^+$, and $Cr(NO)(EHBA)_2$ ($A_{Ram} = 6.6 \times 10^5$ to 9.1×10^5) (Table 2). The g anisotropy for $Cr(NO)(CN)_5^{3-}$, $CrO(EHBA)_2^-$, and CrNTTP ($\Delta g = 0.01-0.04$) is substantially smaller than for $Cr(NO)(H_2O)_5^{2+}$, $Cr(NO)(EHBA)^+$, and $Cr(NO)(EHBA)_2$ ($\Delta g = 0.08$). We therefore attribute the greater effectiveness of the Raman process in spin−lattice relaxation for $Cr(NO)(H_2O)_5^{2+}$, $Cr(NO)(EHBA)^+$, and $Cr(NO)(EHBA)_2$ to the greater spin−orbit coupling in these complexes. Above about 60 K a

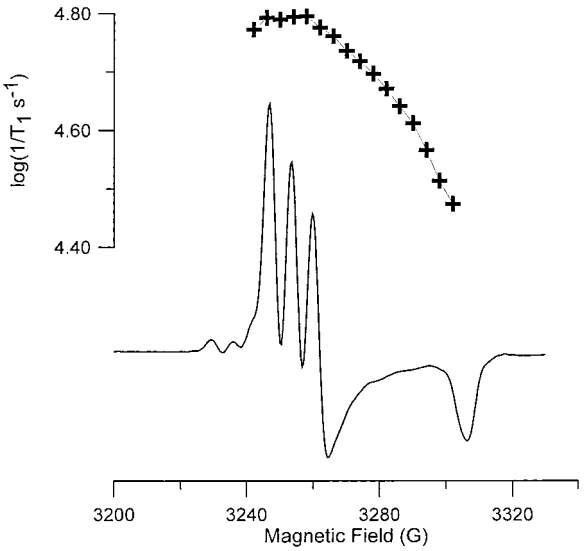

Figure 6. Continuous wave X-band (9.115 GHz) EPR spectrum of 1.5 mM $Cr(NO)(CN)_5^{3-}$ obtained at 100 K with 0.05 mW microwave power and 1.0 G modulation amplitude at 100 kHz and dependence on position in the spectrum for $\log(1/T_1)$ of 0.9 mM $Cr(NO)(CN)_5^{3-}$ at 100 K.

local vibrational mode makes a much larger contribution to the spin−lattice relaxation for $Cr(NO)(CN)_5^{3-}$ than for $Cr(NO)(H_2O)_5^{2+}$, $Cr(NO)(EHBA)^+$, or $Cr(NO)(EHBA)_2$. Significant contributions to spin−lattice relaxation from local modes also were found for $CrO(EHBA)_2^-$ and CrNTTP.[17]

The dependence of $1/T_1$ on position in the CW spectrum of $Cr(NO)(CN)_5^{3-}$ at 100 K is shown in Figure 6. Near the parallel turning point in the spectrum (∼3305 G), $1/T_1$ is about a factor of 2 slower than near the perpendicular turning point. The resolved nitrogen hyperfine splitting near the perpendicular turning point causes this turning point to be spread from about 3245 to 3260 G. Similarly, for the Cr(V) complex CrNTTP at 100 K, $1/T_1$ is about a factor of 2 slower near the parallel turning point than in the perpendicular plane.[1] Both $Cr(NO)(CN)_5^{3-}$ and CrNTTP have approximately C_{4v} local symmetry at the chromium center, and the temperature dependence of the relaxation indicates a major contribution from a local mode at temperatures near 100 K. For $Cr(NO)(EHBA)_2$, $Cr(NO)(EHBA)^+$, and $Cr(NO)(H_2O)_5^{2+}$, the values of $1/T_1$ at 100 K are independent of position in the spectrum, within experimental uncertainty. Similarly $1/T_1$ for the Cr(V) complex $CrO(EHBA)_2^-$ exhibited minimal dependence on position in the spectrum.[3] The observation of an orientation dependence of $1/T_1$ of the C_{4v} complexes but not for the lower-symmetry complexes [$Cr(NO)(EHBA)_2$, $Cr(NO)(EHBA)^+$, and $CrO(EHBA)_2^-$] is consistent with the previously proposed model of electron spin relaxation based on local vibrational modes.[3] The absence of a dependence of $1/T_1$ on position in the spectrum for $Cr(NO)(H_2O)_5^{2+}$ may indicate that the symmetry is lower than C_{4v} due to hydrogen bonding or bending of the nitrosyl group. The absence of orientation dependence for $Cr(NO)(H_2O)_5^{2+}$ also may reflect the fact that the relaxation at 100 K is dominated by the Raman process whereas that for $Cr(NO)(CN)_5^{3-}$ and CrNTTP is dominated by a local mode.

Electronic Structure. Molecular orbital calculations for metal nitrosyls, including chromium nitrosyls, have been performed to interpret the electronic spectra.[9] The calculations and experimental data indicate that the unpaired electron in chromium nitrosyls is in an orbital that is predominantly d_{xy}. The similarity between the g values (Table 1) and the electron spin relaxation rates (Figure 5) of the chromium−nitrosyl complexes and of chromium(V) complexes is consistent with the presence of the single unpaired electron in a molecular orbital with largely d_{xy} character for both types of complex. If electron transfer from the NO to the chromium were complete, the chromium nitrosyls could be viewed as Cr(I) complexes. Although there is extensive metal to ligand electron donation, there also is significant metal to ligand back π-donation[9,19] which makes the assignment of an oxidation state for the metal ambiguous. The $CrNO^{2+}$ unit also can be represented by the notation $\{CrNO\}^5$, indicating that five valence electrons are localized predominantly in this moiety.[23] Chromium−nitrosyls can be formally viewed as low-spin d^5, which suggests a comparison with low-spin Fe(III) complexes, including heme proteins.

For low-spin Fe(III) porphyrins and low-spin Fe(III) methemoglobin, $1/T_1$ at 100 K is of the order of 10^{10} s^{-1},[24,25] which is about 5 orders of magnitude faster than for the chromium−nitrosyl complexes. The similarity in relaxation rates between the small-molecule model complexes and the heme proteins indicates that the low-spin Fe(III) relaxation process is not specific to the protein environment.[24,25] Unlike the chromium−nitrosyl complexes, the single unpaired electron in most low-spin Fe(III) porphyrins and hemes is in the d_{xz} or d_{yz} orbital and there is a low-lying excited state.[26] The lower energies for the d_{xz} and d_{yz} orbitals in the chromium−nitrosyl complexes than for the hemes has been attributed to strong π-bonding between the chromium and nitrosyl.[19] In the low-spin hemes a low-lying excited state may provide a pathway for rapid electron spin relaxation via an Orbach process. However, analysis of the temperature dependence of $1/T_1$ for the low-spin Fe(III) porphyrins and hemes indicates that the characteristic energy of the process that provides the rapid relaxation at temperatures near 100 K does not match with estimates of the energy splitting for the low-lying excited state.[17] Even if the low-lying excited state does not provide a relaxation pathway via an Orbach process, the low-lying excited state gives rise to large spin−orbit coupling and g anisotropy for the low-spin Fe(III) which contributes to the rapid spin−lattice relaxation. This comparison between chromium−nitrosyl complexes and low-spin Fe(III) hemes demonstrates the strong effect of electronic and molecular structure on electron spin relaxation rates.

Acknowledgment. The support of this work by NIH GM21156 (G.R.E. and S.S.E.) and by Research Corporation (Research Corporation: Cottrell College Science Grant C-2816, S.N.M.) is gratefully acknowledged.

IC981063+

(23) Maurya, R. C.; Mishra, D. D. *Synth. React. Inorg. Met. Org. Chem.* **1989**, *19*, 533−537.
(24) Budker, V.; Du, J.-L.; Seiter, M.; Eaton, G. R.; Eaton, S. S. *Biophys. J.* **1995**, *68*, 2531−2542.
(25) Rakowsky, M. H.; More, K. M.; Kulikov, A. V.; Eaton, G. R.; Eaton, S. S. *J. Am. Chem. Soc.* **1995**, *117*, 2049−2057.
(26) Palmer, G. In *Iron Porphyrins*; Lever, A. B. P., Gray, H. B., Eds.; Addison-Wesley: Reading, MA, 1983; Part 2, Chapter 2.
(27) Groves, J. T.; Takahashi, T.; Butler, W. E. *Inorg. Chem.* **1983**, *22*, 884−887.
(28) Buchler, J. W.; Dreher, C.; Lay, K.-L.; Raap, A. *Inorg. Chem.* **1983**, *22*, 879−884.